On the Effectiveness of Small Multicast Switches in Next-Generation Optical Transport Networks

João Pedro[1,2], António Eira[1], Cátia Pinho[1]
[1] Infinera Unipessoal Lda, Rua da Garagem 1, 2790-078 Carnaxide, Portugal
[2] Instituto de Telecomunicações, Instituto Superior Técnico, Avenida Rovisco Pais 1, 1049-001 Lisboa, Portugal
{JPedro, AEira, CPinho}@Infinera.com

***Abstract*—This paper investigates the suitability of small and unamplified multicast switches to cost-effectively realize highly flexible optical transport networks. A comprehensive modelling exercise considering four possible generations of line interfaces, operating at increasingly higher symbol rates, is reported. The simulation results obtained over a reference network topology provide evidence that small and unamplified multicast switches will have little to no effect in limiting the usable network capacity and, as a result, can be exploited to design lower cost contentionless architectures in next-generation optical networks exploiting C- or SuperC-band fiber transmission.**

Keywords—optical transport network, optical interfaces, node architecture, performance evaluation

I. Introduction

The transport network segment continuously experiences the need to scale capacity and increase flexibility to cost-effectively meet growing requirements from cloud computing, machine-to-machine communications, 5G and in the future 6G, just to name a few drivers. Consecutive generations of coherent interfaces have been instrumental to reduce the cost per bit transported and improve spectral efficiency (SE). Although only limited SE improvements are expected, new generations of line interfaces will continue to decrease the cost per bit/s [1]. Developments in reconfigurable optical add/drop multiplexer (ROADM) [2], and control plane technology [3] paved the way to support advanced features in the optical domain, including dynamic service provisioning and optical restoration [4]. A key ROADM architectural requirement to efficiently support these applications is having a colorless, directionless, and (preferably) contentionless (i.e., CDC) add/drop capability [2]–[6], which enables to use any ROADM add/drop port to transmit/receive over any frequency to/from any direction (i.e., degree). However, the roll out of CDC ROADM nodes has been limited, which can be attributed to both the cost and scalability constraints of the multicast switch (MCS) devices used to realize them [6]. Specifically, low-port count MCSs can restrict the maximum number of channels added/dropped at a node, which can hamper the usable network capacity, that is, new service requests can be blocked due to lack of add/drop ports, even if spectrum resources are available. Conversely, high-port count MCS implementations must include Erbium-doped fiber amplifiers (EDFAs) to compensate for additional losses, making them substantially more expensive.

This work investigates how the foreseeable evolution of coherent line interfaces can impact the effectiveness of using small and unamplified MCSs to realize CDC ROADMs. It is well established that upcoming generations of line interfaces will exploit higher symbol rates [1]. Hence, fewer, but wider, optical channels can be transmitted over each fiber link, as line interfaces from consecutive generations are deployed. This can reduce the number of add/drop ports required at the ROADM nodes, improving the scalability of architectures with fewer available add/drop ports. However, it also means that higher power levels per channel are required at the receiver side to guarantee the same performance. Moreover, in the near-term, line systems may natively exploit a wider fiber transmission bandwidth (e.g., SuperC-band), which can, to a certain extent, offset the ROADM scalability benefits of deploying wider channels. As a result, gaining insight on the prospects of small unamplified MCSs in next-generation optical networks requires detailed network simulations that model the combined impact of the ROADM architecture and set of optical channels forecasted to be available with each line interface generation. Simulation results obtained over a reference network for C- and SuperC-band line systems highlight the scenarios where smaller and more cost-effective MCSs can be effectively used to construct a highly flexible and scalable optical transport network.

II. ROADM Architectures

The widespread deployment of ROADM nodes, covering segments as disparate as ultra-long-haul/continental [5] and metro-aggregation [7], highlight their key role as enablers of remotely reconfigurable and flexible optical networks. For architectural characterization, it is typical to consider two main layers of the ROADM: (i) the express layer; and (ii) the add/drop layer. Generically, the express layer is responsible for switching optical channels between different degrees and between each degree and the (local) add/drop layer [1]. The broadcast-and-select (B&S) and the route-and-select (R&S) architectures have been used to realize the express layer. The first comprises an optical splitter at the node ingress and a wavelength selective switch (WSS) at the node egress for each degree, whereas the latter features a pair of WSSs per degree. The B&S architecture has lower cost but higher insertion loss (IL) for medium- to high-nodal degrees than R&S. Higher IL can impact performance, given the need to increase the gain of the EDFAs to compensate for extra losses, leading to more amplified spontaneous emission (ASE) noise being accumulated. Noteworthy, two EDFAs are used per degree in a ROADM – a pre-amplifier at the ingress, to compensate for ingress fiber attenuation, and a booster-amplifier at the egress, to compensate for ROADM losses. Henceforth, for simplicity, a R&S express layer architecture is assumed.

The add/drop layer determines the connectivity between the add/drop (AD) ports, to which line interfaces are attached, and the express layer. Each architecture to realize this layer features a trade-off between flexibility of AD port utilization versus cost and scalability [4]. AD port utilization flexibility underpins the support of several applications, such as optical restoration [8],

This project has received funding from the European Union's Horizon 2020 research and innovation programme B5G-OPEN Project, grant agreement No. 101016663.

978-3-903176-44-7

fast service provisioning [5], dynamic sharing of pre-deployed regenerators [9] and improved spare device management [3]. Realizing a flexible AD port usage requires fitting the ROADM with more complex and/or higher number of devices/cards. This not only increases ROADM cost but can limit how it scales, i.e., the maximum number of AD ports that can be made available, as well as the maximum number of degrees supported [6]. Note that in specific deployments a fiber cross-connect can also be present between line interfaces and client cards [10].

The fixed AD (F-AD) architecture is the least flexible, where each port can only be used to reach a specific degree using a pre-defined (i.e., fixed) frequency slot. The colorless AD (C-AD) architecture relaxes the latter constraint, enabling to use any frequency slot on a given port, but retaining the directionality constraint. The C-AD architecture can be realized with a splitter/combiner connected to the degree's WSS. A pair of EDFAs may need to be included to offset the add and drop losses. Importantly, being able to reach different degrees from the same AD port – the directionless property – is paramount for most of the abovementioned applications, since it enables to reuse a pre-deployed line interface to set up (or re-route) an optical channel intended to another destination node (or using a different routing path). A simple colorless and directionless AD (CD-AD) architecture can be realized, for instance, by having a WSS that connects to every degree's WSS and feeds a splitter/combiner. The combination of this intermediate WSS and splitter/combiner forms an AD group. Albeit additional AD groups can be installed to increase AD port capacity, contention occurs when overlapping frequency slots are meant to be used in AD ports within the same AD group [4], [6].

The most flexible AD layer architecture allows to use each AD port with any available frequency slot and ingress/egress degree irrespective of the other AD ports' utilization. The resulting CDC-AD architecture can be realized with $M \times N$ MCSs [6] or $M \times N$ WSSs [11], where M is the number of device ports available to connect to the express layer WSSs and N is the number of available AD ports of that device. Current CDC-AD ROADM deployments rely on MCSs and, despite the progress being reported in the literature (e.g., see [11]), $M \times N$ WSSs are expected to remain more expensive than MCSs in the foreseeable future. Figure 1 illustrates the main building blocks of a $M \times N$ MCS. It comprises M splitters/combiners with a size of $1 \times N$ each and N optical switches with a size of $M \times 1$. Hence, the number of splitter/combiner components scales with the number of ports available for ROADM degrees, whereas the number of optical switches grows with the intended number of AD ports per MCS. Importantly, the latter number defines the size of the splitters/combiners required, which is the main contributor to the IL of the device. Small port-count MCSs are typically unamplified, as shown in Fig. 1(a), but realizing higher port-count MCSs requires the inclusion of EDFAs, as illustrated in Fig. 1(b). Since a total of M EDFAs are needed to build an amplified MCS, these devices are considerably costlier than unamplified ones.

The scalability of CDC-AD ROADMs depends on the size of the express layer WSSs and the size of the MCSs. The maximum nodal degree is limited by M. Assuming $1 \times S$ express layer WSSs, the maximum number of add/drop ports of a CDC-AD ROADM with nodal degree D is given by:

$$C_{\max} = (S - D + 1) \times N. \tag{1}$$

The maximum AD ratio also depends on the number of channels that can be supported on the fiber links. Assuming a fiber transmission bandwidth B_{fiber} and that optical channels are allocated a frequency slot with width B_{slot}, the maximum AD ratio is determined by:

$$r_{\max} = \begin{cases} min\left\{\frac{C_{\max}}{D \cdot \lfloor B_{\text{fiber}}/B_{\text{slot}} \rfloor}, 1\right\}, & D \le S \\ 0, & D > S \end{cases}, \tag{2}$$

where $\lfloor x \rfloor$ denotes the largest integer equal or smaller than x and $0 \le r_{\max} \le 1$. A $r_{\max} = 1$ means it is possible to scale the ROADM to the extreme case of adding/dropping all the incoming/outgoing channels. Conversely, a small $r_{\max}$ limits the local add/drop of channels and might lead to blocking of optical channels, decreasing the network usable capacity.

This work considers two MCS configurations, all featuring $M = 8$, i.e., supporting ROADMs with a nodal degree of up to 8. One unamplified 8×6 MCS and one amplified 8×24 MCS are assumed. The IL of each MCS is estimated by adding the losses from the splitting ratio and a fixed loss of 3 dB. Hence, the IL is 11 and 17 dB for the 8×6 MCS and 8×24 MCS, respectively.

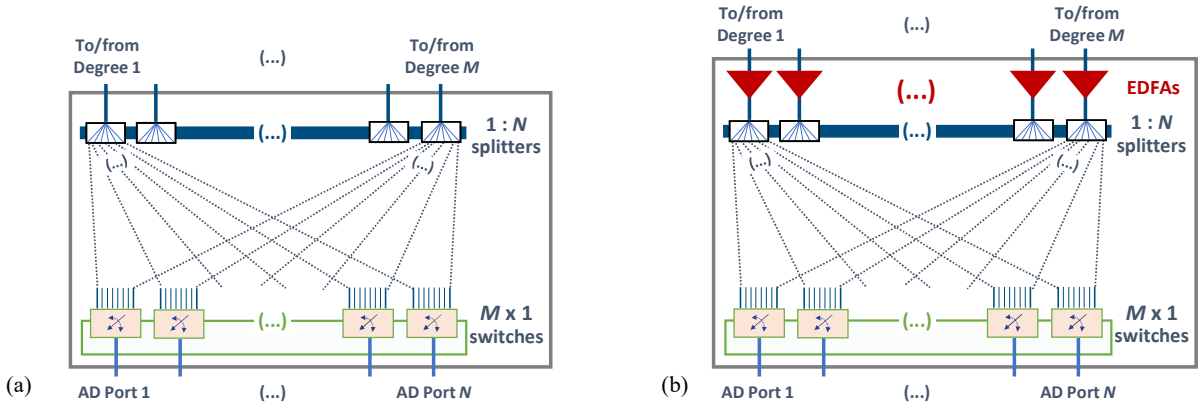

Fig. 1. Multicast switch building blocks in (a) unamplified and (b) amplified configurations.

The express layer comprises 1 × 20 WSSs with IL of 6 dB. The total IL in the express, drop and add paths of the ROADM also account for connector losses between devices. The EDFAs used for the pre-, booster- and add/drop-amplifier are assumed to have a noise figure of 6 dB in the gain regions of interest and their maximum total output power must be observed when calculating the power budget at each ROADM node.

III. Line Interface Evolution

As referred in the previous section, the practical scalability of the ROADM AD layer, estimated by r_{max}, also depends on the maximum number of channels transmitted per fiber. This number increases with the transmission bandwidth exploited by the line system (B_{fiber}) and decreases with the width(s) of the frequency slots used (B_{slot}). The former commonly consists of the C-band's 4.8 THz, with prospects that next-generation line systems will exploit around 6.0 THz in the denominated SuperC-band [12]. The frequency slot width depends on the line interface technology. State-of-the-art interfaces operate at up to 100 Gbaud [12] with a large share of ~70 Gbaud-capable line interfaces already in the field or being deployed [1].

To observe the impact of consecutive generations of line interfaces, an extrapolation exercise was carried out to derive a subset of possible channel formats per generation and the outcome is presented in Table I. The baseline optical channel formats are based on the OpenZR+ multi-source agreement (MSA) [13] and the openROADM MSA [14] for pluggable coherent interfaces. The reference symbol rate (60.1 Gbaud) is suitable to carry Ethernet client signals and includes a 15% FEC [13]. The required optical signal-to-noise ratio (ROSNR) for three different modulation formats is based on OpenZR+, but since the MSA sets conservative values for vendors to comply with, the ROSNR values considered are 1 dB lower. The minimum receiver input power (P_{min}) values for a given penalty in the ROSNR are adapted from the openROADM MSA [14]. Three possible generations of line interfaces are modelled based on the baseline one and assuming ~30 Gbaud symbol rate increase steps. The channel formats' data rate, ROSNR and P_{min} values are scaled accordingly, as shown in Table I. Note that better performance figures (e.g., lower ROSNR) are attained with embedded line interfaces (see [12]) but for the purpose of this analysis interface performance is not the most critical factor.

The frequency slot width for each symbol rate, reported in Table I, is defined as to guarantee optical channels are not significantly impacted by filtering penalties when traversing multiple WSSs [1]. The resulting maximum number of optical channels per fiber is presented in Table II, when considering the C- and SuperC-band. As expected, the maximum fiber channel count decreases as line interfaces exploiting higher symbol rates become available. Figure 2 shows the maximum AD ratio, defined in (2), as a function of the nodal degree when combining the 8 × 6 MCS with 1 × 20 WSSs. As can be seen, the ROADM scalability is significantly impacted by the interface generation. For instance, with the C-band, it is possible to support a r_{max} equal to or above 50% with a nodal degree of 3, 5, 6, and 7, when considering slots widths of 75, 112.5, 150, and 175 GHz, respectively. This suggest that using small unamplified MCSs becomes gradually more competitive as the wider channels introduced by each new generation of line interfaces become available for deployment. Adopting the SuperC-band reduces r_{max} and for the 50% threshold, the largest degree supported in

TABLE II. Maximum Fiber Channel Count

	Slot width [GHz]			
	75	**112.5**	**150**	**175**
C-band (4.8 THz)	64	42	32	27
SuperC-band (6.0 THz)	80	53	40	34

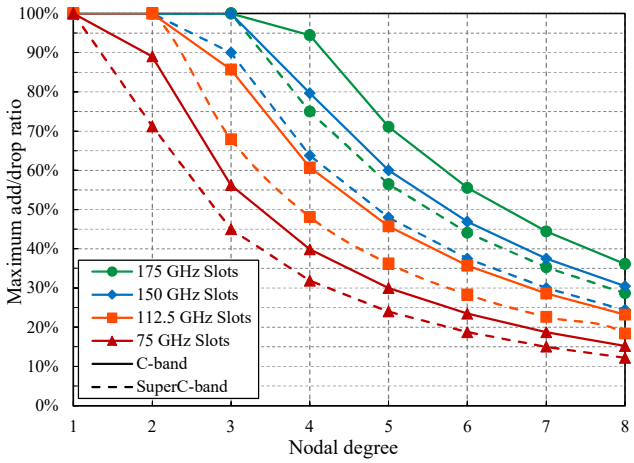

Fig. 2. Maximum AD port ratio with 8 × 6 MCS and 1 × 20 WSS.

TABLE I. Characterization of Four Sets of Optical Channel Formats

Symbol rate [Gbaud]	Mod. format	Data rate [Gb/s]	*ROSNR* [dB]	P_{min} *(0 dB pen.)* [dBm]	P_{min} *(1 dB pen.)* [dBm]	P_{min} *(3 dB pen.)* [dBm]	Slot width [GHz]	SE [b/s/Hz]
60.10	16QAM	400	23	-14	-16	-19	**75**	5.33
	8QAM	300	20	-16	-18	-21		4.00
	QPSK	200	15	-18	-20	-30		2.67
90.15	16QAM	600	24.8	-12	-14	-17	**112.5**	5.33
	8QAM	450	21.8	-14	-16	-19		4.00
	QPSK	300	16.8	-16	-18	-28		2.67
120.20	16QAM	800	26	-11	-13	-16	**150**	5.33
	8QAM	600	23	-13	-15	-18		4.00
	QPSK	400	18	-15	-17	-27		2.67
150.25	16QAM	1000	27	-10	-12	-15	**175**	5.71
	8QAM	750	24	-12	-14	-17		4.29
	QPSK	500	19	-14	-16	-26		2.86

each case is reduced by one. Although not shown here, if the 8 × 24 MCS is used instead, $r_{\max}$ is 100% for all slot widths up to $D = 5$ and between this value and $D = 8$ a decrease of $r_{\max}$ is only noticeable for 75 GHz slots. It must be emphasized that the practical implication of $r_{\max}$ can only be fully evaluated at the network level [4], as investigated in section V.

IV. Network Simulation Setup

To assess the impact of an AD structure in the optical network performance, both a reliable quality of transmission (QoT) estimation model and a comprehensive routing, format selection, spectrum assignment and interface reuse framework are required. This section describes the ones implemented in this work, along with the network topology and traffic pattern utilized in the network simulation exercise.

A. Quality of Transmission Estimation

The baseline QoT estimation model for coherent-detection and phase-modulated signals is given in [12], which assumes both ASE noise from EDFAs and nonlinear interference (NLI) from optical fiber transmission can be approximated as additive white Gaussian noise [15]. Hence, the generalized SNR (GSNR) is equal to $P_S / (P_{ASE} + P_{NLI})$, where P_S is the data signal average power, P_{ASE} is the ASE noise power and P_{NLI} is the NLI contribution to noise. It is also assumed the NLI accumulates incoherently, allowing to assess the GSNR of each fiber span independently from the remaining ones, and that the contribution of self- and cross-phase modulations are accounted for using equations (10) and (11) of [16]. Note that this approach also considers the impact of stimulated Raman scattering (SRS) and has been shown to have good accuracy over a broad transmission spectrum while keeping a reduced computational complexity. The GSNR over a path is given by:

$$GSNR_{tot}^{-1} = \sum_{i=1}^{S} GSNR_i^{-1} + OSNR_{add}^{-1} + OSNR_{drop}^{-1} + (L-1) \cdot OSNR_{int}^{-1} \quad , \tag{3}$$

where S (L) is the number of fiber spans (links) traversed, $GSNR_i$ is the GSNR after transmission along fiber span i, and $OSNR_{add}$, $OSNR_{int}$, and $OSNR_{drop}$ are the OSNR at the add, intermediate, and drop ROADMs, respectively. $GSNR_i$ is maximized by optimizing the launch power using the LOGO strategy [17]. The residual margin at the end of the path is then given by:

$$RM = GSNR_{tot} - ROSNR(P_{Rx}) - M_{sys}, \tag{4}$$

where M_{sys} is a system margin that accounts for the filtering penalties from the cascade of WSSs, the impact of polarization dependent losses and aging margins [12]. Importantly, since performance can be degraded due to having a lower than ideal receiver input power, P_{Rx}, the model has been extended to include the dependence of the ROSNR on this value. Table I shows the power levels for which there is 0, 1 and 3 dB penalty in the ROSNR for each channel format being considered. The value of the ROSNR penalty is linearly interpolated in two segments: $P_{\min}$ *(0 dB penalty)* $< P_{Rx} < P_{\min}$ *(1 dB penalty)* and $P_{\min}$ *(1 dB penalty)* $< P_{Rx} < P_{\min}$ *(3 dB penalty)*. The ROSNR maximum allowed penalty is 3 dB. Note that, amplified MCSs introduce extra ASE noise, lowering the $OSNR_{add}$ and $OSNR_{drop}$.

B. Routing, Format Selection, Spectrum Assignment and Interface Reuse Framework

A multi-period planning framework was implemented to route traffic demands per planning period. The framework is based on [12] but augmented with criteria to optimize the reuse of already deployed, but currently idle, line interfaces with the goal to minimize on-site interventions to change line interface to AD port connections. This feature is particularly relevant in case of ROADMs with AD layer flexibility restrictions [6] and exploited to obtain a sub-set of results described in the next section. The framework utilizes the QoT estimation model described in the previous subsection to determine the feasibility of optical channels over a given routing path in the network.

Within each planning period, traffic demands are ordered by decreasing total number of demands per node pair and routed sequentially. Priority is given to route traffic demands over existing optical channels with available capacity. In case that is not possible, the routing, format selection, spectrum assignment and interface reuse algorithm is tasked with finding the appropriate resources to support the demand. The primary optimization objective of the algorithm is to minimize the number of line interfaces required. It includes a set of secondary optimization objectives that are used to break ties in case more than one solution exists that minimizes the number of line interfaces needed. Particularly, the algorithm will search for the solution(s) that maximizes the number of reused line interfaces (e.g., which have become idle due to traffic churn in previous planning periods), thus minimizing the number of new line interfaces to be deployed. If multiple solutions remain, it will select the one(s) that maximizes spectral efficiency (i.e., giving preference to creating optical channels with higher order modulation formats). The last tie breaking criteria consist of choosing the solution that maximizes AD port reuse (i.e., giving preference to reusing line interfaces that do not require changing the AD port to which they are connected). Note that the last step to break ties is not relevant in CDC ROADMs.

Best Fitted Capacity with Optimized Interface Reuse (BFC-OIR) algorithm	
Input:	Unrouted demand set D, demand being routed d, set of K paths Π_d, MCh format list Φ, where $\Delta(\phi)$ is the spectral efficiency of $\phi \in \Phi$.
1.	Select all unrouted demands between same node pair as d, D'.
2.	For each path and MCh format pair (π, ϕ), with $\pi \in \Pi_d$, $\phi \in \Phi$:
2.1	Create an auxiliary graph G' with nodes representing the ROADMs over π and links representing feasible MChs (with $RM \geq 0$ and available continuous and contiguous spectrum). Set link cost according to number of line interfaces required to carry D'.
2.2	Compute the lowest cost path over the auxiliary graph G', which is characterized by a total interface count $\Omega(\pi, \phi)$.
3.	Shortlist the lowest cost solutions, i.e., the one(s) with minimum $\Omega(\pi, \phi)$. Break ties by selecting the solution with (1) maximum line interface reuse, (2) maximum spectral efficiency $\Delta(\phi)$, and (3) maximum AD port reuse.
Output:	Routing path π^* and MCh format ϕ^* that minimize interface count and specific interfaces that can be reused are selected to support d.

The algorithm considers K candidate routing paths ($K = 3$ in this work) and when setting up new optical channels, spectrum assignment is realized with the first-fit algorithm. In addition, spectrum conversion at intermediate sites is allowed, but only if line interfaces have to be deployed for signal regeneration.

C. Reference Network Topology and Traffic Pattern

The reference topology utilized is the Spanish backbone network (SBN) defined by Telefónica in [18], covering Spain via 30 ROADM nodes. Nodal degree varies between 3 and 5 (average of 3.73). The average span and link lengths are 68 and 148 km, respectively. All spans are standard single mode fiber with attenuation coefficient of 0.21 dB/km, dispersion parameter of 16.8 ps/nm/km, non-linear coefficient of 1.07 W^{-1}/km and a Raman gain of 0.43 $(W\times km\times Hz)^{-1}$. A total of 1dB excess loss at input and output of optical fibers and an extra loss of 0.1 dB/km to account for splice losses, are also assumed to achieve a more accurate modelling of a typical fiber plant. The multi-period network simulation exercise assumes 100 GbE traffic demands are generated according to the traffic spatial distribution in [18]. The network lifecycle comprises 20 planning periods and 50% traffic churn. The described framework to set up traffic demands is used per planning period and without awareness of the traffic demands in later periods. Different average offered traffic load values are considered. All results reported are the average value obtained from running 20 independent simulation runs.

V. Results and Discussion

The simulation results reported in this section assume CDC ROADMs with 1 × 20 WSSs in the express layer and 8 × 6 or 8 × 24 MCSs in the AD layer. Additional simulations were done with C-AD ROADMs using 1 × 10 splitter/combiners. It was observed that, in average, 45% of the line interface reuse events with C-AD architecture, which take place when traffic churn allows to release an interface and reuse it to set up new optical channels, require on-site interventions to change the AD port to which the interface is connected. This highlights the importance of CDC-AD ROADMs to minimize operational expenses, since interfaces can always be reused without any AD port change.

Figure 3 depicts both the average carried traffic load and the average blocked traffic load as a function of the offered traffic load in the SBN exploiting the C-band, Fig. 3(a), and the SuperC-band, Fig. 3(b). In both plots, using 75 GHz slots (i.e., 60 Gbaud interfaces) results in higher blocking when the ROADMs are equipped with 8 × 6 MCSs, but not when they have 8 × 24 MCSs instead. The additional blocking with the smaller MCS is due to AD port shortage, that is, the lack of AD ports in some of the nodes leads to blocking traffic demands. Conversely, with the larger MCS, blocking only occurs due to the lack of available spectrum resources. It can be observed that when the SuperC-band is exploited, a slight increase of blocking is also visible with 112.5 GHz slots (90 Gbaud interfaces) and 8 × 6 MCSs. With the larger slot widths (120 and 150 Gbaud interfaces), using 8 × 6 MCSs leads to the same carried traffic load as that obtained with the larger amplified 8 × 24 MCSs. Table III presents the average offered traffic load that results in a target blocking probability P_B = 1%. When using the 8 × 24 MCSs around 27% more traffic load can be offered if SuperC-band is used instead of C-band. Similar increases are observed for 8 × 6 MCSs with the wider frequency slots, with a minor reduction to a 23% gain observed when using 112.5 GHz slots. When employing the 8 × 6 MCS and 75 GHz slots the same offered traffic load is attained for both fiber transmission bands, which is 20% (C-band) and 36% (SuperC-band) below that obtained when the larger MCS is employed. This shows that for the smallest slot width the lack of available AD ports becomes the dominant source of blocking when using the smaller MCS.

The key benefit of consecutive generations of coherent line interfaces is evident in Fig. 4(a), which shows how the number of line interfaces required is reduced as interfaces operating at higher symbol rates are introduced. Moreover, Fig. 4(b) depicts the number of required MCSs as a function of the offered traffic

TABLE III. Network Average Traffic Load for P_B = 1%

		Slot width [GHz]			
		75	**112.5**	**150**	**175**
C-band	8 × 6 MCS	141 Tb/s	163 Tb/s	161 Tb/s	159 Tb/s
	8 × 24 MCS	176 Tb/s	163 Tb/s	162 Tb/s	160 Tb/s
SuperC-band	8 × 6 MCS	141 Tb/s	201 Tb/s	206 Tb/s	204 Tb/s
	8 × 24 MCS	222 Tb/s	208 Tb/s	206 Tb/s	204 Tb/s

TABLE IV. MCS Hardware Requirements for T = 135 Tb/s

		Slot width [GHz]			
		75	**112.5**	**150**	**175**
8 × 6 MCS	1 × 6 splitters	784	592	496	424
	8 × 1 switches	588	444	372	318
8 × 24 MCS	1 × 24 splitters	240	208	168	136
	8 × 1 switches	720	624	504	408
	EDFAs	240	208	168	136

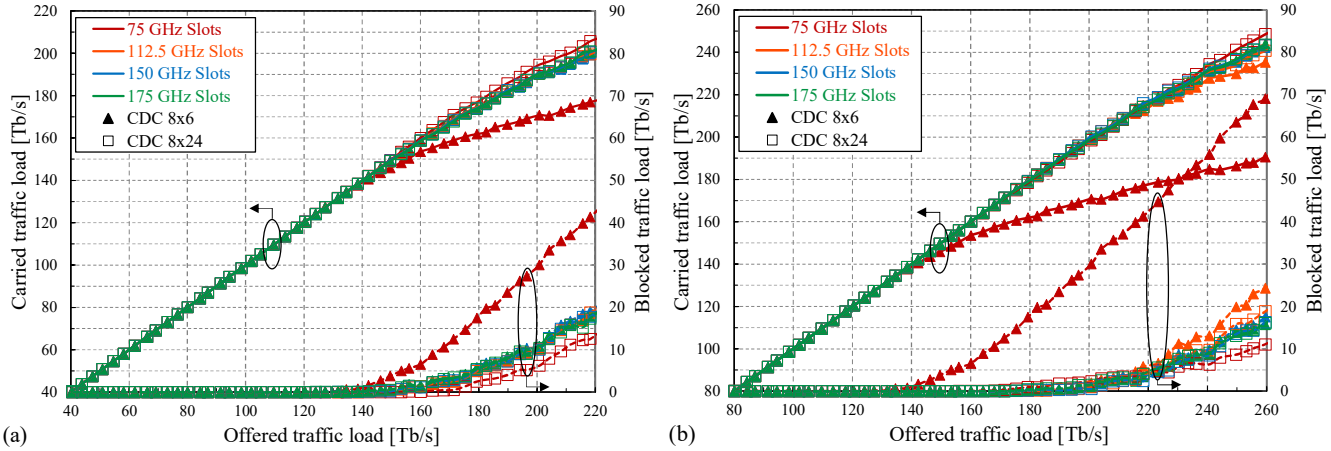

Fig. 3. Average carried and blocked traffic load in SBN topology exploiting (a) the C-band and (b) the SuperC-band.

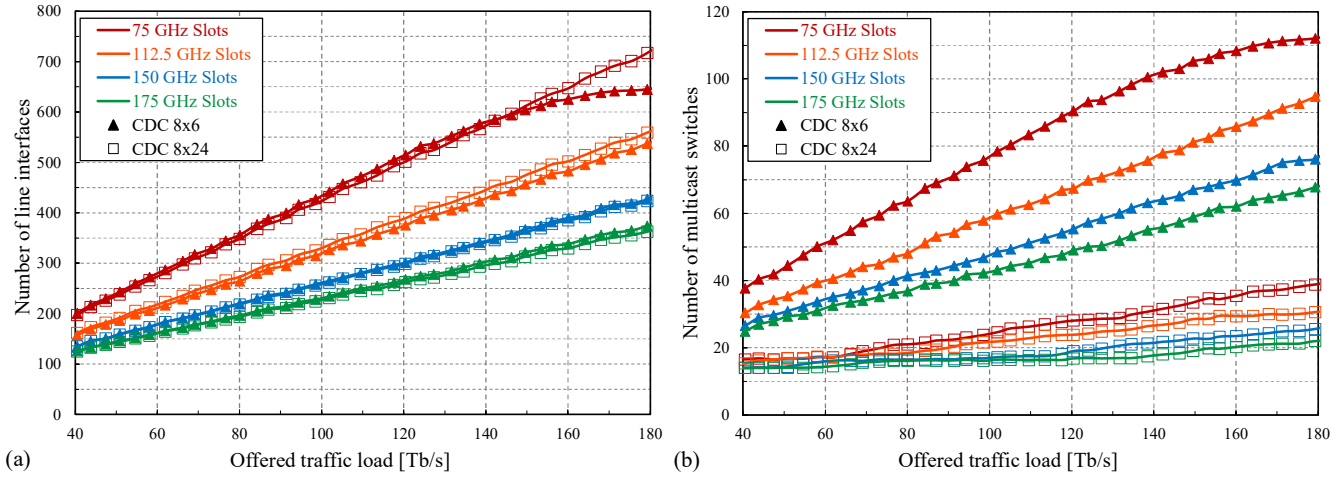

Fig. 4. Average number of (a) line interfaces and (b) multicast switches in SBN topology with SuperC-band.

load. As can be seen, an additional benefit of next-generation line interfaces is reducing the number of AD ports used and, hence, the number of MCSs required. The plot also shows that, as expected, fewer MCSs are needed if the larger 8 × 24 devices are used. However, although each of these MCSs has 4× the number of AD ports of the 8 × 6 MCS, the savings in number of MCSs observed when using the larger devices instead of the smaller ones are significantly below that factor. Particularly, up to 3× times the number of MCSs are needed when relying on the 8 × 6 MCS instead of the 8 × 24 MCS. This can be explained by the fact that smaller MCSs allow more granular increments in number of AD ports, enabling a better match between in use and deployed AD ports. Table IV shows the MCS hardware requirements for a target offered traffic load T = 135 Tb/s and includes the total number of splitter/combiners, switches and EDFAs needed. It can be observed that 8 × 24 MCSs not only demand a large number of EDFAs, which are not required with 8 × 6 MCSs, but also between 22 and 40% more optical switches than the smaller MCSs. These figures highlight that adopting small unamplified MCSs to realize CDC ROADMs results in a significantly more cost-effective network solution.

VI. Conclusions and Outlook

This paper introduced a network simulation framework to evaluate the impact of deploying CDC ROADMs based on small unamplified multicast switches in transport networks exploiting increasingly higher symbol rates. Simulation results obtained in a reference network topology with C- and Super-C band line systems provide evidence that increasing line interface symbol rates above 90 Gbaud decreases the add/drop ports requirements to such extent that using smaller unamplified multicast switches does not lead to additional blocking when loading the network. Since these devices save EDFAs and optical switches, when compared to using larger and amplified multicast switches, they are shown to be an attractive solution to scale-up capacity.

References

[1] J. Pedro, N. Costa, and S. Pato, "Optical transport network design beyond 100 Gbaud [Invited]," J. Optical Commun. and Netw., vol. 12, no. 2, pp. A123-A134, 2020.

[2] S. Gringeri, B. Basch, V. Shukla, R. Egorov, and T. Xia, "Flexible architectures for optical transport nodes and networks," IEEE Commun. Mag., vol. 48, no. 7, pp. 40-50, 2010.

[3] B. Bathula, A. Chiu, R. Sinha, and S. Woodward, "Routing and regenerator planning in a carrier's core ROADM network," in Proc. of 2017 Optical Fiber Comm. (OFC) Conf., March 2017, paper Th4F.4.

[4] J. Pedro, and S. Pato, "Impact of add/drop port utilization flexibility in DWDM networks [Invited]," J. Optical Commun. and Netw., vol 4, no. 11, pp. B142-B150, 2012.

[5] S. Woodward, M. Feuer, I. Kim, P. Palacharla, X. Wang, and D. Bihon, "Service velocity: rapid provisioning strategies in optical ROADM networks," J. Optical Commun. and Netw., vol 4, no. 2, pp. 92-98, 2012.

[6] J. Pedro, and S. Pato, "On the value proposition of the contentionless add/drop ROADM property in DWDM transport networks," in Proc. of 16th Intern. Conf. on Transparent Optical Netw. (ICTON), July 2014, paper Tu.A1.2.

[7] J. Hernández, M. Quagliotti, L. Serra, L. Luque, R. Silva, A. Rafel, et al., "Comprehensive model for technoeconomic studies of next-generation central offices for metro networks," J. Optical Commun. and Netw., vol. 12, no. 12, pp. 414-427, 2020.

[8] A. Eira, J. Pedro, and J. Pires, "Modeling cost versus flexibility in optical transport networks," J. Lightw. Technol., vol. 37, no. 1, pp. 61-74, 2019.

[9] J. Pedro, "Predeployment of regenerators for fast service provisioning in DWDM transport networks [Invited]," J. Optical Commun. and Netw., vol 7, no. 2, pp. A190-A199, 2015.

[10] I. Kim, P. Palacharla, X. Wang, D. Bihon, M. Feuer, and S. Woodward, "Performance of colorless, non-directional ROADMs with modular client-side fiber cross-connects," in Proc. of 2012 Optical Fiber Comm. (OFC) Conf., March 2012, paper NM3F.7.

[11] P. Colbourne, S. McLaughlin, C. Murley, S. Gaudet, and D. Burke, "Contentionless twin 8x24 WSS with low insertion loss," in Proc. of 2018 Optical Fiber Comm. (OFC) Conf., March 2018, paper Th4A.1.

[12] J. Pedro, N. Costa, and S. Sanders, "Cost-effective strategies to scale the capacity of regional optical transport networks," J. Optical Commun. and Netw., vol 14, no. 2, pp. A154-A165, 2022.

[13] OpenZR+ MSA, https://openzrplus.org/

[14] Open ROADM MSA, http://openroadm.org/

[15] P. Poggiolini, "The GN model of non-linear propagation in uncompensated coherent optical systems," J. Lightw. Technol., vol. 30, no. 24, pp. 3857-3879, 2012.

[16] D. Semrau, R. Killey, and P. Bayvel, "A closed-form approximation of the Gaussian noise model in the presence of inter-channel stimulated Raman scattering," J. Lightw. Technol., vol. 37, no. 9, pp. 1924-1936, 2019.

[17] P. Poggiolini, G. Bosco, A. Carena, R. Cigliutti, V. Curri, F. Forghieri, et. al., "The LOGON strategy for low-complexity control plane implementation in new-generation flexible networks," in Proc. of 2013 Optical Fiber Comm. (OFC) Conf., March 2013, paper OW1H.3.

[18] FP7 IDEALIST project deliverable D1.1 – Elastic Optical Network Architecture: reference scenario, cost and planning, cordis.europa.eu/docs/projects/cnect/9/317999/080/deliverables/001-D11ElasticOpticalNetworkArchitecture.doc